
What Can the Neural Tangent Kernel Tell Us About Adversarial Robustness?

Anonymous Author(s)

Affiliation

Address

email

Abstract

1 Adversarial vulnerability of neural nets, and subsequent techniques to create robust
2 models have attracted significant attention; yet we still lack a full understand-
3 ing of this phenomenon. Here, we study adversarial examples of trained neural
4 networks through analytical tools afforded by recent theory advances connecting
5 neural networks and kernel methods, namely the Neural Tangent Kernel (NTK),
6 following a growing body of work that leverages the NTK approximation to suc-
7 cessfully analyze important deep learning phenomena and design algorithms for
8 new applications. We show how NTKs allow to generate adversarial examples in a
9 “training-free” fashion, and demonstrate that they transfer to fool their finite-width
10 neural net counterparts in the “lazy” regime. We leverage this connection to provide
11 an alternative view on robust and non-robust features, which have been suggested
12 to underlie the adversarial brittleness of neural nets. Specifically, we define and
13 study features induced by the eigendecomposition of the associated kernel to better
14 understand the role of robust and non-robust features, the reliance on both for
15 standard classification and the robustness-accuracy trade-off. We find that such
16 features are surprisingly consistent across architectures, and that robust features
17 tend to correspond to the largest eigenvalues of the model, and thus are learned
18 early during training. Our framework allows us to identify and visualize non-robust
19 yet useful features. Finally, we shed light on the robustness mechanism underlying
20 adversarial training of neural nets used in practice: quantifying the evolution of
21 the associated empirical NTK, we demonstrate that its dynamics falls much earlier
22 into the “lazy” kernel regime and manifests a much stronger form of the well
23 known bias to prioritize learning features within the top eigenspaces of the kernel,
24 compared to standard training.

25 1 Introduction

26 Despite the tremendous success of deep neural networks in many computer vision and language
27 modeling tasks, as well as in scientific discoveries, their properties and the reasons for their success
28 are still poorly understood. Focusing on computer vision, a particularly surprising phenomenon
29 evidencing that those machines drift away from how humans perform image recognition is the
30 presence of *adversarial examples*, images that are almost identical to the original ones, yet are
31 misclassified by otherwise accurate models.

32 Since their discovery [41], a vast amount of work has been devoted to understanding the sources of
33 adversarial examples and explanations include, but are not limited to, the close to linear operating
34 mode of neural nets [21], the curse of dimensionality carried by the input space [21, 39], insufficient
35 model capacity [31, 43] or spurious correlations found in common datasets [23]. In particular,
36 one widespread viewpoint is that adversarial vulnerability is the result of a model’s sensitivity to
37 imperceptible yet well-generalizing features in the data, so called *useful non-robust* features, giving

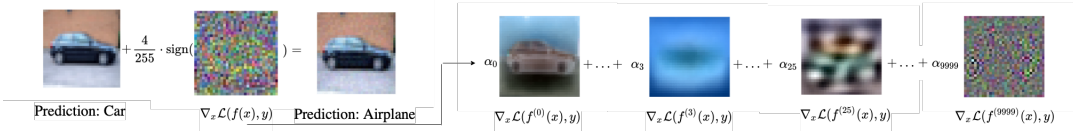


Figure 1: **Left.** Standard setup of an adversarial attack, where a barely perceivable perturbation is added to an image to confuse an accurate classifier. **Right.** The correspondence between neural networks and kernel machines allows to visualize a decomposition of this perturbation, each part attributed to a different feature of the model. The first few features tend to be *robust*.

38 rise to a trade-off between accuracy and robustness [43, 45]. This gradual understanding has enabled
 39 the design of training algorithms, that provide convincing, yet partial, remedies to the problem; the
 40 most prominent of them being adversarial training and its many variants [16, 21, 30]. Yet we are far
 41 from a mature, unified theory of robustness that is powerful enough to universally guide engineering
 42 choices or defense mechanisms.

43 In this work, we aim to get a deeper understanding of adversarial robustness (or lack thereof) by
 44 focusing on the recently established connection of neural networks with kernel machines. Infinitely
 45 wide neural networks, trained via gradient descent with infinitesimal learning rate, provably become
 46 kernel machines with a data-independent, but architecture dependent kernel - its Neural Tangent
 47 Kernel (NTK) - that remains constant during training [4, 24, 27, 28]. The analytical tools afforded by
 48 the rich theory of kernels have resulted in progress in understanding the optimization landscape and
 49 generalization capabilities of neural networks [3, 17], together with the discovery of interesting deep
 50 learning phenomena [18, 34], while also inspiring practical advances in diverse areas of applications
 51 such as the design of better classifiers [38], efficient neural architecture search [14], low-dimensional
 52 tasks in graphics [42] and dataset distillation [32]. While the NTK approximation is increasingly
 53 utilized, even for finite width neural nets, little is known about the adversarial robustness properties
 54 of these infinitely wide models.

55 **Our contribution:** Our work inscribes itself into the quest to leverage analytical tools afforded by
 56 kernel methods, in particular spectral analysis, to track properties of interest in the associated neural
 57 nets, in this case as they pertain to robustness. We study adversarial perturbations and robustness
 58 of kernels so as to enrich our understanding of adversarial robustness in general machine learning
 59 models. To this end, we first demonstrate that adversarial perturbations generated *analytically* with
 60 the NTK can successfully lead the associated trained wide neural networks (in the kernel-regime)
 61 to misclassify, thus allowing kernels to faithfully predict the lack of robustness of those trained
 62 neural networks. In other words, adversarial (non-) robustness transfers from kernels to networks;
 63 and adversarial perturbations generated via kernels resemble those generated by the corresponding
 64 trained networks. One implication of this transferability is that we can analytically devise adversarial
 65 examples that do not require access to the trained model and in particular its weights; instead these
 66 “blind spots” may be calculated a-priori, before training starts. Although similar transferability has
 67 already been known and exploited in prior work that trains substitute models, we demonstrate that this
 68 notion holds from first principles that only require the a-priori description of the model architecture.
 69 The analytical expressions afforded by the kernel might provide a better understanding of the elusive
 70 concept of transferability also across architectures, as the corresponding expressions for the associated
 71 kernels can be compared directly.

72 A perhaps even more crucial implication of the NTK approach to robustness relates to the *understand-*
 73 *ing* of adversarial examples. Indeed, we show how the spectrum of the NTK provides an alternative
 74 way to define *features* of the model, to classify them according to their robustness and usefulness
 75 and visually inspect them via their contribution to the adversarial perturbation (see Fig. 1). This
 76 in turn allows us to verify previously conjectured properties of standard classifiers; dependence on
 77 both *robust* and *non-robust* features in the data [43], and tradeoff of accuracy and robustness during
 78 training. In particular we observe that features tend to be rather invariable across architectures, and
 79 that robust features tend to correspond to the *top* of the eigenspectrum (see Fig. 2), and as such are
 80 learned first by the corresponding wide nets [3, 24]. Moreover, we are able to visualize useful non-
 81 robust features of standard models (Fig. 5). While this conceptual feature distinction has been highly
 82 influential in recent works that study the robustness of deep neural networks [1, 25, 40], to the best of
 83 our knowledge, none of them has explicitly demonstrated the dependence of networks on such feature
 84 functions (except for simple linear models [20]). Rather, these works either reveal such features in
 85 some indirect fashion, or accept their existence as an assumption. Here, we show that Neural Tangent

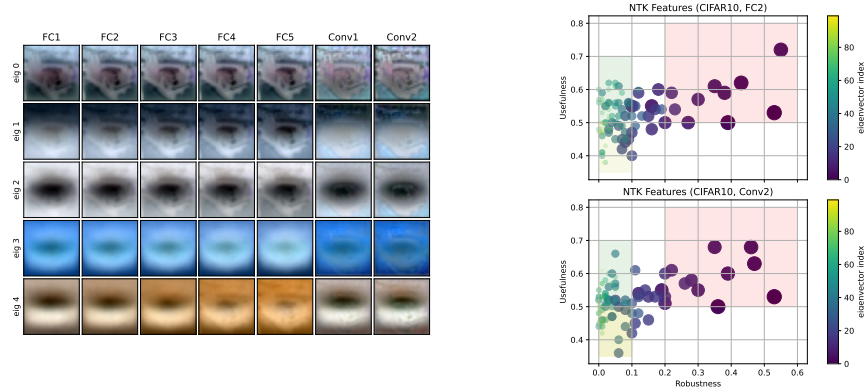


Figure 2: **Left:** Top 5 features for 7 different kernel architectures for a car image extracted from the CIFAR10 dataset when trained on car and plane images. **Right:** Features according to their robustness (x-axis) and usefulness (y-axis). Larger/darker bullets correspond to larger eigenvalues. *Useful* features have > 0.5 -usefulness; shaded boxes are meant to help visualize useful-robust regions.

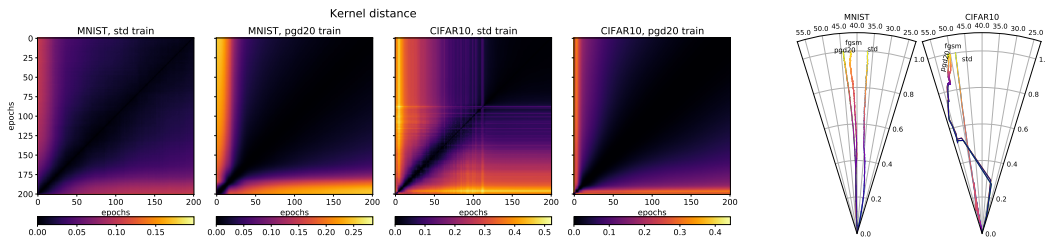


Figure 3: **Left:** Kernel rotation during standard, and adversarial training. Left to right: MNIST, standard, MNIST adversarial, CIFAR standard, CIFAR adversarial. **Right:** Kernel trajectories in polar space for MNIST (left) and CIFAR10 (right). Darker colors indicate earlier epochs.

86 Kernel theory endows us with a natural definition of features through its eigen-decomposition and
 87 provides a way to *visualise and inspect robust and non-robust features directly* on the function space
 88 of trained neural networks.

89 Interestingly, this connection also enables us to empirically demonstrate that robust features of
 90 standard models alone are not enough for robust classification. Aiming to understand, then, what
 91 makes robust models robust, we track the *evolution* of the data-dependent *empirical* NTK during
 92 *adversarial training* of neural networks used in practice. Prior experimental work has found that
 93 networks with non-trivial width to depth ratio which are trained with large learning rates, depart from
 94 the NTK regime and fall in the so-called “rich feature” regime, where the NTK changes substantially
 95 during training [7, 18, 19, 34]. In our work, which to the best of our knowledge is the first to
 96 provide insights on how the kernel behaves during adversarial training, we find that the NTK evolves
 97 much faster compared to standard training, simultaneously both changing its features and assigning
 98 more importance to the more robust ones, giving direct insight into the mechanism at play during
 99 adversarial training (see Fig. 3). In summary, the contributions of our work are the following:

- 100 • We discuss how to generate adversarial examples for infinitely-wide neural networks via the
 101 NTK, and show that they transfer to fool their associated (finite width) nets in the appropriate
 102 regime, yielding a “training-free” attack without need to access model weights (Sec. 3).
- 103 • We then turn to the kernel machines corresponding to infinitely-wide networks trained
 104 with small learning rate to deepen our understanding of adversarial robustness. Using the
 105 spectrum of the NTK, we give an alternative definition of features, providing a natural
 106 decomposition or perturbations into robust and non-robust parts [23, 43] (Fig. 1). We
 107 confirm that robust features overwhelmingly correspond to the top part of the eigenspectrum;
 108 hence they are learned early on in training. We bolster previously conjectured hypotheses
 109 that prediction relies on both robust and non-robust features and that robustness is traded for
 110 accuracy during standard training. Further, we show that only utilizing the robust features of
 111 standard models is not sufficient for robust classification (Sec. 4).

112 • We turn to finite-width neural nets with standard parameters to study the *dynamics* of their
 113 empirical NTK during *adversarial training*. We show that the kernel rotates in a way that
 114 enables both new (robust) feature learning and that drastically increases of the importance
 115 (relative weight) of the robust features over the non-robust ones. We further highlight
 116 the structural differences of the kernel change during adversarial training versus standard
 117 training and observe that the kernel seems to enter the “lazy” regime much faster (Sec. 5).

118 Collectively, our findings may help explain many phenomena present in the adversarial ML literature
 119 and further elucidate both the vulnerability of standard models and the robustness of adversarially
 120 trained ones. We provide code to visualize features induced by kernels, giving a unique and principled
 121 way to inspect features induced by standardly trained nets.

122 **Related work:** To the best of our knowledge the only prior work that leverages NTK theory to derive
 123 perturbations in some adversarial setting is due to [44], yet with entirely different focus. It deals
 124 with what is coined *generalization attacks*: the process of altering the training data distribution to
 125 prevent models to generalise on clean data. [6] study aspects of robust models through their linearized
 126 sub-networks, but do not leverage NTKs. Our work is the first to provide a kernel-induced notion of
 127 features and to study robustness in adversarial training in the NTK regime.

128 2 Preliminaries

129 We introduce background material and definitions important to our analysis. Here, we restrict
 130 ourselves to binary classification and scalar kernels, to keep notation light. We defer the multiclass
 131 case, complete definitions and a more detailed discussion of prior work to the Appendix.

132 2.1 Adversarial Examples

133 Let f be a classifier, \mathbf{x} be an input (e.g. a natural image) and y its label (e.g. the image class). Then,
 134 given that f is an accurate classifier on \mathbf{x} , $\tilde{\mathbf{x}}$ is an adversarial example [41] for f if 1) their distance
 135 $d(\mathbf{x}, \tilde{\mathbf{x}})$ is small. Common choices in computer vision are the ℓ_p norms, especially the ℓ_∞ norm on
 136 which we focus henceforth, and 2) $f(\tilde{\mathbf{x}}) \neq y$. That is, the perturbed input is being misclassified.

137 Given a loss function \mathcal{L} , such as cross-entropy, one can construct an adversarial example $\tilde{\mathbf{x}} = \mathbf{x} + \boldsymbol{\eta}$
 138 by finding the perturbation $\boldsymbol{\eta}$ that produces the maximal increase of the loss, solving

$$\boldsymbol{\eta} = \arg \max_{\|\boldsymbol{\eta}\|_\infty \leq \epsilon} \mathcal{L}(f(\mathbf{x} + \boldsymbol{\eta}), y), \quad (1)$$

139 for some $\epsilon > 0$ that quantifies the dissimilarity between the two examples. In general, this is a
 140 non-convex problem and one can resort to first order methods [21]

$$\tilde{\mathbf{x}} = \mathbf{x} + \epsilon \cdot \text{sign}(\nabla_{\mathbf{x}} \mathcal{L}(f(\mathbf{x}), y)), \quad (2)$$

141 or iterative versions for solving it [26, 30]. The former method is usually called *Fast Gradient Sign*
 142 *Method (FGSM)* and the latter *Projected Gradient Descent (PGD)*. These methods are able to produce
 143 examples that are being misclassified by common neural networks with a probability that approaches
 144 1 [12]. Even more surprisingly, it has been observed that adversarial examples crafted to “fool” one
 145 machine learning model are consistently capable of “fooling” others [35, 36], a phenomenon that
 146 is known as the *transferability* of adversarial examples. Finally, *adversarial training* refers to the
 147 alteration of the training procedure to include adversarial samples for teaching the model to be robust
 148 [21, 30] and empirically holds as the strongest defense against adversarial examples [30, 45].

149 2.2 Robust and Non-Robust features

150 Despite a vast amount of research, the reasons behind the existence of adversarial examples are
 151 not perfectly clear. A line of work has argued that a central reason is the presence of robust and
 152 non-robust features in the data that standard models learn to rely upon [23, 43]. In particular it
 153 is conjectured that reliance on *useful but non-robust* features during training is responsible for the
 154 brittleness of neural nets. Here, we slightly adapt the feature definitions of [23]¹, and extend them to
 155 multi-class problems (see Appendix).

¹We distinguish useful and robust features based on their accuracy as classifiers, not in terms of correlation with the labels as in [23], allowing a natural extension to the multi-class setting. For robustness, we consider any accuracy bounded away from zero as robust, quantifying that an adversary cannot drive accuracy to zero entirely.

156 Let \mathcal{D} be the data generating distribution with $x \in \mathcal{X}$ and $y \in \{\pm 1\}$. We define a *feature* as a function
 157 $\phi : \mathcal{X} \rightarrow \mathbb{R}$ and distinguish how they perform as classifiers. Fix $\rho, \gamma \geq 0$:

158 1. **ρ -Useful** feature: A feature ϕ is called ρ -*useful* if

$$\mathbb{E}_{x,y \sim \mathcal{D}} [\mathbf{I}_{\{\text{sign}[\phi(x)] = y\}}] = \rho \quad (3)$$

159 2. **γ -Robust** feature: A feature ϕ is called γ -*robust* if it remains useful under any perturbation
 160 inside a bounded "ball" \mathcal{B} , that is if

$$\mathbb{E}_{x,y \sim \mathcal{D}} \left[\inf_{\delta \in \mathcal{B}} \mathbf{I}_{\{\text{sign}[\phi(x+\delta)] = y\}} \right] = \gamma \quad (4)$$

161 In general, a feature adds predictive value if it gives an advantage above guessing the most likely
 162 label, i.e. $\rho > \max_{y' \in \{\pm 1\}} \mathbb{E}_{x,y \sim \mathcal{D}} [\mathbf{I}_{\{y' = y\}}]$, and we will speak of "useful" features in this case,
 163 omitting the ρ . We will call such a feature **useful, non-robust** if it is useful, but γ -robust only for
 164 $\gamma = 0$ or very close to 0, depending on context.

165 The vast majority of works imagines features as being induced by the *activations* of neurons in
 166 the net, most commonly those of the penultimate layer (*representation-layer* features), but this
 167 formal definition is in no way restricted to activations, and we will show how to exploit it using
 168 the eigenspectrum of the NTK. In particular, in Sec. 4, we demonstrate that the above framework
 169 agrees perfectly with features induced by the eigenspectrum of the NTK of a network, providing a
 170 natural way to decompose the predictions of the NTK into such feature functions. In particular we
 171 can identify robust, useful, and, indeed, useful non-robust features.

172 2.3 Neural Tangent Kernel

173 Let $f : \mathbb{R}^d \rightarrow \mathbb{R}$ be a (scalar) neural network with a linear final layer parameterized by a set of
 174 weights $\mathbf{w} \in \mathbb{R}^p$ and $\{\mathcal{X}, \mathcal{Y}\}$ be a dataset of size n , with $\mathcal{X} \in \mathbb{R}^{n \times d}$ and $\mathcal{Y} \in \{\pm 1\}^n$. Linearized
 175 training methods study the first order approximation

$$f(\mathbf{x}; \mathbf{w}_{t+1}) = f(\mathbf{x}; \mathbf{w}_t) + \nabla_{\mathbf{w}} f(\mathbf{x}; \mathbf{w}_t)^\top (\mathbf{w}_{t+1} - \mathbf{w}_t). \quad (5)$$

176 The network gradient $\nabla_{\mathbf{w}} f(\mathbf{x}; \mathbf{w}_t)$ induces a kernel function $\Theta_t : \mathbb{R}^d \times \mathbb{R}^d \rightarrow \mathbb{R}$, usually referred as
 177 the *Neural Tangent Kernel (NTK)* of the model

$$\Theta_t(\mathbf{x}, \mathbf{x}') = \nabla_{\mathbf{w}} f(\mathbf{x}; \mathbf{w}_t)^\top \nabla_{\mathbf{w}} f(\mathbf{x}'; \mathbf{w}_t). \quad (6)$$

178 This kernel describes the dynamics with infinitesimal learning rate (gradient flow). In general, the
 179 tangent space spanned by the $\nabla_{\mathbf{w}} f(\mathbf{x}; \mathbf{w}_t)$ twists substantially during training, and learning with the
 180 Gram matrix of Eq. (6) (empirical NTK) corresponds to training along an intermediate tangent plane.
 181 Remarkably, however, in the infinite width limit with appropriate initialization and low learning rate,
 182 it has been shown that f becomes a *linear* function of the parameters [24, 28], and the NTK remains
 183 *constant* ($\Theta_t = \Theta_0 =: \Theta$). Then, for learning with ℓ_2 loss the training dynamics of infinitely wide
 184 networks admits a closed form solution corresponding to kernel regression [4, 24, 27]

$$f_t(\mathbf{x}) = \Theta(\mathbf{x}, \mathcal{X})^\top \Theta^{-1}(\mathcal{X}, \mathcal{X}) (I - e^{-\lambda \Theta(\mathcal{X}, \mathcal{X}) t}) \mathcal{Y}, \quad (7)$$

185 where $\mathbf{x} \in \mathbb{R}^d$ is any input (training or testing), t denotes the time evolution of gradient descent,
 186 λ is the (small) learning rate and, slightly abusing notation, $\Theta(\mathcal{X}, \mathcal{X}) \in \mathbb{R}^{n \times n}$ denotes the matrix
 187 containing the pairwise training values of the NTK, $\Theta(\mathcal{X}, \mathcal{X})_{ij} = \Theta(\mathbf{x}_i, \mathbf{x}_j)$, and similarly for
 188 $\Theta(\mathbf{x}, \mathcal{X}) \in \mathbb{R}^n$. To be precise, Eq. (7) gives the *mean* output of the network using a weight-
 189 independent kernel with variance depending on the initialization².

190 3 Transfer results in the kernel regime

191 In this section, we show how to generate adversarial examples from NTKs and discuss their similarity
 192 to the ones generated by the actual networks. Note that for network results, we restrict ourselves to
 193 wide networks initialized in the "lazy" regime with small learning rates (the "kernel regime").

²For that reason, in the experiments, we often compare this with the centered prediction of the actual neural network, $f - f_0$, as is commonly done in similar studies [15].

194 **3.1 Generation of Adversarial Examples for Infinitely Wide Neural Networks**

195 Adversarial examples arise in the context of *classification*, while the NTK learning process is
 196 described by a regression as in Eq. (7). The arguably simplest way to align with the framework
 197 presented in Eq. (1) is to treat the outputs of the kernel similar to logits of a neural net, mapping them
 198 to a probability distribution via the sigmoid/softmax function and apply cross-entropy loss.

199 A simple calculation (see Appendix, together with the generalization to the multi-class case) gives:

200 *The optimal one step adversarial example of a scalar, infinitely wide, neural network is given by*

$$\tilde{\mathbf{x}} = \mathbf{x} - y\epsilon \cdot \text{sign}(\nabla_{\mathbf{x}} f_t(\mathbf{x})), \quad (8)$$

201 for $\|\tilde{\mathbf{x}} - \mathbf{x}\|_{\infty} \leq \epsilon$, where $\nabla_{\mathbf{x}} f_t(\mathbf{x}) = \nabla_{\mathbf{x}} \Theta(\mathbf{x}, \mathcal{X})^{\top} \Theta^{-1}(\mathcal{X}, \mathcal{X})(I - e^{-\lambda \Theta(\mathcal{X}, \mathcal{X}) t}) \mathcal{Y}$.

202 One can conceive other ways to generate adversarial perturbations for the kernel, either by changing
 203 the loss function (as previously done in neural networks (e.g. [12])) or through a Taylor expansion
 204 around the test input, and we present such alternative derivations in the Appendix. However, in
 205 practice we observe little difference between that approach and the one presented here.

206 **3.2 Transfer results and kernel attacks**

207 Predictions from NTK theory for infinitely wide neural networks have been used successfully for their
 208 large finite width counterparts, so it seems reasonable to conjecture that adversarial perturbations
 209 generated via the kernel as in Eq. (8) strongly resemble those directly computed for the corresponding
 210 neural net as per Eq. (2). In particular, this would imply that adversarial perturbations derived from
 211 the NTK should not only fool the kernel machine itself, but also lead wide neural nets to misclassify.
 212 While similar transfer results in different contexts have been observed indirectly, via the *effects* of
 213 the perturbation on metrics like accuracy [32, 44], we aim to look deeper to compare perturbations
 214 *directly*. High similarity would imply that *any* gradient based white-box attack on the neural net can
 215 be successfully mimicked by a “black-box” kernel derived attack.

216 **Setting.** To this end, we train multiple two-layer neural networks on
 217 image classifications tasks extracted from MNIST and CIFAR-10
 218 and compare adversarial examples generated by Eqs. (2) (attacking
 219 the neural network) and (8) (attacking the kernel). The networks
 220 are trained with small learning rate and are sufficiently large, so lie
 221 close to the NTK regime. We track cosine similarity between the
 222 gradients of the loss from the NTK predictions and the gradients
 223 from the actual neural net as training evolves. Then, we generate
 224 adversarial perturbations from both the neural net and the kernel
 225 machine, and test whether those produced by the latter can fool the
 226 former. Full experimental details can be found in the Appendix.

227 **Results.** Our experiments confirm a very strong alignment of loss
 228 gradients from the neural nets and the NTK across the whole dura-
 229 tion of training, as can be seen in Fig. 4 (top). Then, as expected,
 230 kernel-generated attacks produce a similar drop in accuracy through-
 231 out training as the networks “own” white-box attacks, eventually
 232 driving robust accuracy to 0%, as seen in Fig. 4 (bottom). We re-
 233 produce these plots for MNIST in the Appendix, leading to similar
 234 conclusions.

235 When concerned with security aspects of neural nets, adversarial
 236 attacks are mainly characterised as either *white-box* or *black-box*
 237 attacks [36]. White box attacks assume full access to the neural
 238 network and in particular its weights; prominent examples include FGSM/PGD attacks. Black box
 239 attacks, on the other hand, can only *query* the model to try to infer the loss gradient, either through
 240 training separate surrogate models [35] or through carefully crafted input-output pairs fed to the
 241 target model [2, 13, 22]. NTK theory and the experiments of this section suggest a threat model in
 242 which the attacker does not require access to the model or its weights, nor training of a substitute
 243 model. For fixed architecture and training data, all the information required for the computation of
 244 (8) is available at initialization, making the “NTK-attack” akin to a “training free” substitution attack,
 245 and, at least in the kernel-regime for wide nets considered here, as effective as white-box attacks.

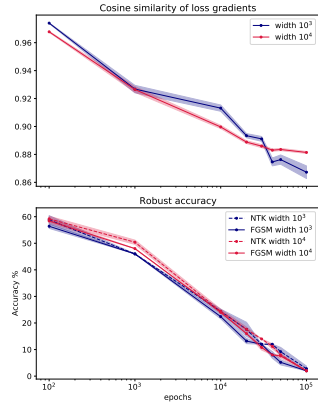


Figure 4: **Top.** Cosine similarity between the loss gradient of the neural net and of the NTK prediction for the same time point. **Bottom.** Robust accuracy of neural net against its own adversarial examples (solid) and corresponding NTK examples (dashed). CIFAR10, car vs plane.

246 **4 NTK eigenvectors induce robust and non-robust features**

247 This close connection between adversarial perturbations from the kernel and the corresponding neural
 248 net gives us the opportunity to bring to bear kernel tools on the study of adversarial robustness and its
 249 relation to features in a more direct fashion. Several recent works leverage properties of the NTK,
 250 and specifically its spectrum, to study aspects of approximation and generalization in neural networks
 251 [3, 8, 9, 10]. Here we show how the spectrum relates to robustness and helps to clarify the notion of
 252 robust/non-robust features.

253 We define *features* induced by the eigendecomposition of the Gram matrix $\Theta(\mathcal{X}, \mathcal{X}) = \sum_{i=1}^n \lambda_i \mathbf{v}_i \mathbf{v}_i^\top$.
 254 We will be most interested in the *end* of training, when the model has access to all the features it can
 255 extract from the training data \mathcal{X} . As $t \rightarrow \infty$, Eq. (7) becomes $f_\infty(\mathbf{x}) = \Theta(\mathbf{x}, \mathcal{X})^\top \Theta(\mathcal{X}, \mathcal{X})^{-1} \mathcal{Y}$
 256 and can be decomposed as $f_\infty(\mathbf{x}) = \Theta(\mathbf{x}, \mathcal{X})^\top \sum_{i=1}^n \lambda_i^{-1} \mathbf{v}_i \mathbf{v}_i^\top \mathcal{Y} = \sum_{i=1}^n f^{(i)}(\mathbf{x})$, where

$$f^{(i)} : \mathbb{R}^d \rightarrow \mathbb{R}^k, f^{(i)}(\mathbf{x}) := \lambda_i^{-1} \Theta(\mathbf{x}, \mathcal{X})^\top \mathbf{v}_i \mathbf{v}_i^\top \mathcal{Y}. \quad (9)$$

257 Each $f^{(i)}$ can be seen as a *unique feature* captured from the (training) data. Note that these functions
 258 map the input to the output space, thus matching the definitions of Sec. 2.2. Also observe that
 259 all $f^{(i)}$'s jointly recover the original prediction of the model, while each one, intuitively, should
 260 contribute something different to it.

261 Importantly, these features induce a decomposition of the gradient of the loss into parts, each
 262 representing gradients of a unique feature as already advertised in Fig. 1. The binary case is
 263 particularly elegant as it gives rise to a linear decomposition of the gradient as

$$\nabla_{\mathbf{x}} \mathcal{L}(f_\infty(\mathbf{x}), y) = \sum_{i=1}^n \alpha_i \nabla_{\mathbf{x}} \mathcal{L}(f^{(i)}(\mathbf{x}), y), \quad (10)$$

264 for some α_i depending on \mathbf{x} and y (see Appendix). But if $f^{(i)}$'s are features, how do they look like?

265 **Feature properties of common architectures:** With these
 266 definitions in place, we can now analyze the characteristics
 267 of features for commonly used architectures, leveraging their
 268 associated NTK. To be consistent with the previous section, we
 269 consider classification problems from MNIST (10 classes) and
 270 CIFAR-10 (car vs airplane). We compose the Gram matrices
 271 from the whole training dataset (50000 and 10000, respectively),
 272 and compute the different feature functions $f^{(i)}$ using the eigen-
 273 decomposition of the matrix. We estimate the **usefulness** of a
 274 feature $f^{(i)}$ by measuring its accuracy on a hold-out validation
 275 set, and its **robustness** by perturbing each input of this set,
 276 using an FGSM attack on feature $f^{(i)}$. We consider several
 277 different Fully Connected and Convolutional Kernels, whose
 278 expressions are available through the Neural Tangents library
 279 [33], built on top of JAX [11]. We summarize our findings on
 280 how these features behave:

281 *Functions $f^{(i)}$ represent visually distinct features.* We visualise each feature $f^{(i)}$ by plotting its
 282 gradient with respect to \mathbf{x} . Fig. 2 shows the gradient of the first 5 features for various architectures
 283 for a specific image from the CIFAR-10 dataset. We observe that features are fairly consistent across
 284 models, and they are interpretable: for example the 4th feature seems to represent the dominant color of
 285 an image, while the 5th one seems to be capturing horizontal edges.

286 *Networks use both robust and non-robust features for prediction.* It has been speculated that neural
 287 networks trained in a standard (non adversarial) fashion rely on both robust and non-robust features.
 288 Our feature definition in Eq. (9) shows that this is indeed the case. The NTK of common neural
 289 networks consists of both robust features that match human expectations, such as the ones depicted in
 290 Fig. 2, but also on features that are predictive of the true label, while not being robust to adversarial
 291 perturbations of the input (Fig. 5). Fig. 2 depicts the first 100 features of a fully connected and a
 292 convolutional tangent kernel in Usefulness-Robustness space. The upper left region of the plots shows
 293 a large amount of useful, yet non-robust features. These features seem random to human observers.

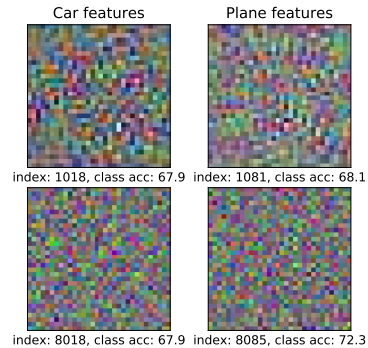


Figure 5: Non-robust, useful features earlier and later in the spectrum, for CIFAR10 car and plane.

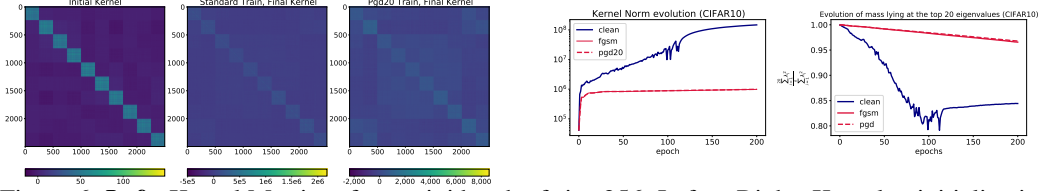


Figure 6: **Left:** Kernel Matrices for a mini batch of size 256. Left to Right: Kernel at initialization, Kernel after standard training, Kernel after adversarial training (20 pgd steps). The standard kernel grows significantly more than the adversarial one. **Right:** (a) Kernel Frobenius norm evolution, and (b) concentration on the top 20 eigenvalues during standard and adversarial training. Setting: CIFAR10, $\ell_\infty = 8/255$.

294 *Robustness lies at the top.* We observe in Fig. 2 that features corresponding to the top eigenvectors
 295 tend to be robust. This is consistent among different models and between the two datasets (see
 296 Appendix). Since these eigenvectors are the ones fitted first during training [3, 24], it is no wonder
 297 that the loss gradient evolves from coherence to noise, as observed in Fig. A1. This also explains the
 298 apparent trade-off between robustness and accuracy of neural networks as training progresses: useful,
 299 robust features are fitted first, followed by useful, but non-robust ones. This ties in well with both
 300 empirical findings [37] and theoretical case studies [8, 9, 10] that demonstrate that low frequency
 301 *functions* are fitted first during training and provide favorable generalization properties and we would
 302 associate robust features with these low-frequency parts.

303 *Robust features alone are not enough.* In light of these findings, it might be reasonable to conjecture
 304 that we could obtain robust models by retaining the robust features of the prediction, while discarding
 305 the non-robust ones. The spectral approach gives a principled way to disentangle features and create
 306 kernel machines keeping only the robust ones. Our results show that in general it is not possible to
 307 obtain non-trivial performance without compromising robustness in this fashion, strengthening the
 308 case for the necessity of data augmentation in the form of adversarial training (see the Appendix for
 309 an in-depth study).

310 5 Kernel dynamics during adversarial training

311 Given the apparent necessity for adversarial training to produce robust models, how does it achieve
 312 this goal? To shed some light on this fundamental question, we depart from the “lazy” NTK regime
 313 and study the evolution of the NTK of adversarially trained models. For a neural network trained
 314 with gradient descent, as the learning rate $\eta \rightarrow 0$, the continuous time dynamics can be written as

$$\frac{\partial w}{\partial t} = -\eta \nabla_w \mathcal{L} = -\eta \nabla_w f^\top \frac{\partial \mathcal{L}}{\partial f} \quad \text{and} \quad \frac{\partial f}{\partial t} = -\eta \underbrace{\nabla_w f \nabla_w f^\top}_{\Theta_t} \frac{\partial \mathcal{L}}{\partial f}. \quad (11)$$

315 In the NTK regime, this kernel Θ_t remains fixed at its initial value. However, outside this regime, it
 316 has been demonstrated, both empirically [7, 18, 19, 34] and theoretically [5], that Θ_t is not constant
 317 during training, and is changing as the weights move. In adversarial training, moreover, there is the
 318 additional effect that at each weight update, the data changes as well. For that reason, understanding
 319 the dynamics of adversarial training requires tracking the evolution of a kernel $\Theta_t(\mathcal{X}_t, \mathcal{X}_t)$, where
 320 \mathcal{X}_t denotes the current (mini) batch of training data. Notice that the tangent vector $\nabla_w f(\mathcal{X}_t)$ is still
 321 describing the instantaneous change of f on the current batch of data, thus $\Theta_t(\mathcal{X}_t, \mathcal{X}_t)$ is informative
 322 of the local geometry of the function space, justifying its value as a quantity to be measured during
 323 adversarial training.

324 We train a deep convolutional architecture on CIFAR-10 (multiclass) with standard (sgd) and adver-
 325 sarial training using PGD with an ℓ_∞ constraint. Full implementations details and accuracy curves
 326 can be found in the Appendix, together with the reproduction of the same experiment on MNIST,
 327 where the observations are similar. We track the following quantities during training:

Kernel distance. We compare two kernels using a *scale invariant distance*, which quantifies the
 relative rotation between them, as used in other works studying NTK dynamics (e.g. [18]):

$$d(\Theta_i, \Theta_j) = 1 - \frac{\text{Tr}(\Theta_i \Theta_j^\top)}{\sqrt{\text{Tr}(\Theta_i \Theta_i^\top)} \sqrt{\text{Tr}(\Theta_j \Theta_j^\top)}}.$$

328 **Polar dynamics.** Zooming in on the change that the initial kernel undergoes, we define a *polar space*
 329 on which we measure the movement of the kernel:

$$r_t = \frac{\|\Theta_t - \Theta_0\|_F}{\|\Theta_f - \Theta_0\|_F}, \quad \theta_t = \arccos(1 - d(\Theta_t, \Theta_0)), \quad (12)$$

330 where Θ_0, Θ_f are the initial and final kernel, respectively. Fig. 3 presents a heatmap of kernel
 331 distances at different time steps for both standard and adversarial training, as well as both training
 332 trajectories in polar space.

333 **Concentration on subspaces.** To quantify weight concentration on the top region of the spectrum,
 334 we track the (normalized) Frobenius norm of subspaces as $\sum_{i=1}^p \lambda_i^2 / \sum_{i=1}^n \lambda_i^2$, for various cut-offs p ,
 335 where we have indexed the eigenvalues from largest to smallest. Fig. 6 depicts concentration on the
 336 top 20 eigenvalues during training.

337 Our findings show that similar to what has been reported in prior work [18], the kernel rotates
 338 significantly in the beginning of training and then slows down for both standard and adversarial
 339 training. However, in the latter case, this second phase begins a lot earlier. As Fig. 3 illuminates,
 340 the kernel moves a greater distance than when performing standard training, but after a few epochs
 341 it stops both rotating and expanding; note that this is not the case for standard training where the
 342 kernel increases its magnitude substantially later in training, and in fact grows to have a norm orders
 343 of magnitude larger than during adversarial training (see Fig. 6). In hindsight, this behavior is
 344 perhaps not surprising, as each element of the kernel measures similarity between data points, and
 345 a robust machine should be more conservative when estimating similarity. The observation that
 346 during adversarial training the kernel becomes relatively static relatively fast might indicate that
 347 *linear* dynamics govern the later phase of adversarial training. It has been observed in previous
 348 works [18, 19, 34] that linearization after a few initial epochs of rapid rotation often closely matches
 349 performance of full network training. Our results indicate that a similar phenomenon occurs even
 350 under the data shift of adversarial training, opening avenues to design robust machines more efficiently.

351 Moreover, endowed with the knowledge that at least for kernels trained with static data robust features
 352 lie at the top, we study polar dynamics of the top space only (see Appendix) to observe that there is
 353 substantial rotation in this space, suggesting that robust features are learned early on not only during
 354 standard, but in particular during adversarial training. Even more interestingly, Fig. 6 demonstrates
 355 that not only the robust features change, but their relative weight as measured by the concentration on
 356 the top-20 space is increasing simultaneously relative to standard training as well, and remains large;
 357 in fact, significantly larger than during standard training. As each eigenvalue weights the importance
 358 of the corresponding feature on the final prediction, this implies that the kernel “learns” to depend
 359 more on the most robust features.

360 Put together, these findings reveal different kernel dynamics during standard and adversarial training:
 361 the kernel rotates much faster, expands much less and becomes “lazy” much earlier than during
 362 standard training. Fully understanding the properties of converged adversarial kernels remains an
 363 important avenue for future work, that might allow to design faster algorithms for robust classification.

364 6 Final Remarks

365 We have studied adversarial robustness through the lens of the NTK across multiple architectures
 366 and data sets both in the idealized NTK regime and the “rich feature” regime. When connecting the
 367 spectrum of the kernel with fundamental properties characterizing robustness our phenomenological
 368 study reveals a universal picture of the emergence of robust and non-robust features and their role
 369 during training. There are certain limitations and unexplored themes in our work; Sec. 3 argues that
 370 transferable attacks from the NTK may be as effective as white-box attacks, but this warrants an
 371 in-depth study across architectures, kernels and data sets (which has not been the main focus of this
 372 work). Sec. 4 visualises features for fairly simple models, since the computation of kernel derivatives
 373 is a costly procedure. It would be interesting to use our framework to visualise features from more
 374 complicated architectures. Finally, our work in Sec. 5 invites more research on the kernel at the end
 375 of adversarial training, similar to what has been done for standard models [29].

376 We hope that our viewpoint can motivate further theoretical understanding of adversarial phenomena
 377 (such as transferability) and the design of better and/or faster adversarial learning algorithms, by
 378 further analyzing the kernels from robust deep neural networks.

References

- 379
- 380 [1] Z. Allen-Zhu and Y. Li. Feature purification: How adversarial training performs robust deep
381 learning. *2021 IEEE 62nd Annual Symposium on Foundations of Computer Science (FOCS)*,
382 pages 977–988, 2022.
- 383 [2] M. Andriushchenko, F. Croce, N. Flammarion, and M. Hein. Square attack: A query-efficient
384 black-box adversarial attack via random search. In A. Vedaldi, H. Bischof, T. Brox, and J. Frahm,
385 editors, *Computer Vision - ECCV 2020 - 16th European Conference, Glasgow, UK, August*
386 *23-28, 2020, Proceedings, Part XXIII*, volume 12368 of *Lecture Notes in Computer Science*,
387 pages 484–501. Springer, 2020.
- 388 [3] S. Arora, S. Du, W. Hu, Z. Li, and R. Wang. Fine-Grained Analysis of Optimization and
389 Generalization for Overparameterized Two-Layer Neural Networks. In K. Chaudhuri and
390 R. Salakhutdinov, editors, *Proceedings of the 36th International Conference on Machine*
391 *Learning*, volume 97 of *Proceedings of Machine Learning Research*, pages 322–332. PMLR,
392 09–15 Jun 2019.
- 393 [4] S. Arora, S. S. Du, W. Hu, Z. Li, R. Salakhutdinov, and R. Wang. On exact computation with
394 an infinitely wide neural net. In H. M. Wallach, H. Larochelle, A. Beygelzimer, F. d’Alché-Buc,
395 E. B. Fox, and R. Garnett, editors, *Advances in Neural Information Processing Systems 32:*
396 *Annual Conference on Neural Information Processing Systems 2019, NeurIPS 2019, December*
397 *8-14, 2019, Vancouver, BC, Canada*, pages 8139–8148, 2019.
- 398 [5] A. Atanasov, B. Bordelon, and C. Pehlevan. Neural networks as kernel learners: The silent
399 alignment effect. In *International Conference on Learning Representations*, 2022.
- 400 [6] Y. Bai, X. Yan, Y. Jiang, S. Xia, and Y. Wang. Clustering effect of adversarial robust models. In
401 M. Ranzato, A. Beygelzimer, Y. N. Dauphin, P. Liang, and J. W. Vaughan, editors, *Advances*
402 *in Neural Information Processing Systems 34: Annual Conference on Neural Information*
403 *Processing Systems 2021, NeurIPS 2021, December 6-14, 2021, virtual*, pages 29590–29601,
404 2021.
- 405 [7] A. Baratin, T. George, C. Laurent, R. D. Hjelm, G. Lajoie, P. Vincent, and S. Lacoste-Julien.
406 Implicit regularization via neural feature alignment. In A. Banerjee and K. Fukumizu, editors,
407 *The 24th International Conference on Artificial Intelligence and Statistics, AISTATS 2021, April*
408 *13-15, 2021, Virtual Event*, volume 130 of *Proceedings of Machine Learning Research*, pages
409 2269–2277. PMLR, 2021.
- 410 [8] R. Basri, D. W. Jacobs, Y. Kasten, and S. Kritchman. The convergence rate of neural networks
411 for learned functions of different frequencies. In H. M. Wallach, H. Larochelle, A. Beygelzimer,
412 F. d’Alché-Buc, E. B. Fox, and R. Garnett, editors, *Advances in Neural Information Processing*
413 *Systems 32: Annual Conference on Neural Information Processing Systems 2019, NeurIPS*
414 *2019, December 8-14, 2019, Vancouver, BC, Canada*, pages 4763–4772, 2019.
- 415 [9] R. Basri, M. Galun, A. Geifman, D. W. Jacobs, Y. Kasten, and S. Kritchman. Frequency bias
416 in neural networks for input of non-uniform density. In *Proceedings of the 37th International*
417 *Conference on Machine Learning, ICML 2020, 13-18 July 2020, Virtual Event*, volume 119 of
418 *Proceedings of Machine Learning Research*, pages 685–694. PMLR, 2020.
- 419 [10] A. Bietti and J. Mairal. On the inductive bias of neural tangent kernels. In H. M. Wallach,
420 H. Larochelle, A. Beygelzimer, F. d’Alché-Buc, E. B. Fox, and R. Garnett, editors, *Advances*
421 *in Neural Information Processing Systems 32: Annual Conference on Neural Information*
422 *Processing Systems 2019, NeurIPS 2019, December 8-14, 2019, Vancouver, BC, Canada*, pages
423 12873–12884, 2019.
- 424 [11] J. Bradbury, R. Frostig, P. Hawkins, M. J. Johnson, C. Leary, D. Maclaurin, G. Necula, A. Paszke,
425 J. VanderPlas, S. Wanderman-Milne, and Q. Zhang. JAX: composable transformations of
426 Python+NumPy programs, 2018. URL <http://github.com/google/jax>.
- 427 [12] N. Carlini and D. A. Wagner. Towards evaluating the robustness of neural networks. In *2017*
428 *IEEE Symposium on Security and Privacy, SP 2017, San Jose, CA, USA, May 22-26, 2017*,
429 pages 39–57. IEEE Computer Society, 2017.

- 430 [13] P. Chen, H. Zhang, Y. Sharma, J. Yi, and C. Hsieh. ZOO: zeroth order optimization based black-
431 box attacks to deep neural networks without training substitute models. In B. M. Thuraisingham,
432 B. Biggio, D. M. Freeman, B. Miller, and A. Sinha, editors, *Proceedings of the 10th ACM*
433 *Workshop on Artificial Intelligence and Security, AISec@CCS 2017, Dallas, TX, USA, November*
434 *3, 2017*, pages 15–26. ACM, 2017.
- 435 [14] W. Chen, X. Gong, and Z. Wang. Neural architecture search on imagenet in four GPU hours: A
436 theoretically inspired perspective. In *9th International Conference on Learning Representations,*
437 *ICLR 2021, Virtual Event, Austria, May 3-7, 2021*. OpenReview.net, 2021.
- 438 [15] L. Chizat, E. Oyallon, and F. R. Bach. On lazy training in differentiable programming. In
439 H. M. Wallach, H. Larochelle, A. Beygelzimer, F. d’Alché-Buc, E. B. Fox, and R. Garnett,
440 editors, *Advances in Neural Information Processing Systems 32: Annual Conference on Neural*
441 *Information Processing Systems 2019, NeurIPS 2019, December 8-14, 2019, Vancouver, BC,*
442 *Canada*, pages 2933–2943, 2019.
- 443 [16] F. Croce, M. Andriushchenko, V. Sehwag, E. Debenedetti, N. Flammarion, M. Chiang, P. Mittal,
444 and M. Hein. Robustbench: a standardized adversarial robustness benchmark. In *Thirty-fifth*
445 *Conference on Neural Information Processing Systems Datasets and Benchmarks Track (Round*
446 *2)*, 2021.
- 447 [17] S. S. Du, J. D. Lee, H. Li, L. Wang, and X. Zhai. Gradient descent finds global minima of
448 deep neural networks. In K. Chaudhuri and R. Salakhutdinov, editors, *Proceedings of the 36th*
449 *International Conference on Machine Learning, ICML 2019, 9-15 June 2019, Long Beach,*
450 *California, USA*, volume 97 of *Proceedings of Machine Learning Research*, pages 1675–1685.
451 PMLR, 2019.
- 452 [18] S. Fort, G. K. Dziugaite, M. Paul, S. Kharaghani, D. M. R. 0001, and S. Ganguli. Deep learning
453 versus kernel learning: an empirical study of loss landscape geometry and the time evolution of
454 the neural tangent kernel. In H. Larochelle, M. Ranzato, R. Hadsell, M.-F. Balcan, and H.-T.
455 Lin, editors, *Advances in Neural Information Processing Systems 33: Annual Conference on*
456 *Neural Information Processing Systems 2020, NeurIPS 2020, December 6-12, 2020, virtual,*
457 *2020*.
- 458 [19] M. Geiger, S. Spigler, A. Jacot, and M. Wyart. Disentangling feature and lazy training in deep
459 neural networks. *Journal Of Statistical Mechanics-Theory And Experiment*, 2020(11):113301,
460 2020.
- 461 [20] G. Goh. A discussion of ‘adversarial examples are not bugs, they are features’: Two ex-
462 amples of useful, non-robust features. *Distill*, 2019. [https://distill.pub/2019/advex-bugs-](https://distill.pub/2019/advex-bugs-discussion/response-3)
463 [discussion/response-3](https://distill.pub/2019/advex-bugs-discussion/response-3).
- 464 [21] I. J. Goodfellow, J. Shlens, and C. Szegedy. Explaining and harnessing adversarial examples. In
465 Y. Bengio and Y. LeCun, editors, *3rd International Conference on Learning Representations,*
466 *ICLR 2015, San Diego, CA, USA, May 7-9, 2015, Conference Track Proceedings*, 2015.
- 467 [22] A. Ilyas, L. Engstrom, A. Athalye, and J. Lin. Black-box adversarial attacks with limited queries
468 and information. In J. G. Dy and A. Krause, editors, *Proceedings of the 35th International*
469 *Conference on Machine Learning, ICML 2018, Stockholmsmässan, Stockholm, Sweden, July*
470 *10-15, 2018*, volume 80 of *Proceedings of Machine Learning Research*, pages 2142–2151.
471 PMLR, 2018.
- 472 [23] A. Ilyas, S. Santurkar, D. Tsipras, L. Engstrom, B. Tran, and A. Madry. Adversarial examples
473 are not bugs, they are features. In H. M. Wallach, H. Larochelle, A. Beygelzimer, F. d’Alché-
474 Buc, E. B. Fox, and R. Garnett, editors, *Advances in Neural Information Processing Systems 32:*
475 *Annual Conference on Neural Information Processing Systems 2019, NeurIPS 2019, December*
476 *8-14, 2019, Vancouver, BC, Canada*, pages 125–136, 2019.
- 477 [24] A. Jacot, C. Hongler, and F. Gabriel. Neural tangent kernel: Convergence and generalization in
478 neural networks. In S. Bengio, H. M. Wallach, H. Larochelle, K. Grauman, N. Cesa-Bianchi, and
479 R. Garnett, editors, *Advances in Neural Information Processing Systems 31: Annual Conference*
480 *on Neural Information Processing Systems 2018, NeurIPS 2018, December 3-8, 2018, Montréal,*
481 *Canada*, pages 8580–8589, 2018.

- 482 [25] J. Kim, B.-K. Lee, and Y. M. Ro. Distilling robust and non-robust features in adversarial
483 examples by information bottleneck. In A. Beygelzimer, Y. Dauphin, P. Liang, and J. W.
484 Vaughan, editors, *Advances in Neural Information Processing Systems*, 2021.
- 485 [26] A. Kurakin, I. J. Goodfellow, and S. Bengio. Adversarial examples in the physical world. In
486 *5th International Conference on Learning Representations, ICLR 2017, Toulon, France, April*
487 *24-26, 2017, Workshop Track Proceedings*, 2017.
- 488 [27] J. Lee, L. Xiao, S. Schoenholz, Y. Bahri, R. Novak, J. Sohl-Dickstein, and J. Pennington.
489 Wide Neural Networks of Any Depth Evolve as Linear Models Under Gradient Descent. In
490 H. Wallach, H. Larochelle, A. Beygelzimer, F. d'Alché-Buc, E. Fox, and R. Garnett, editors,
491 *Advances in Neural Information Processing Systems*, volume 32. Curran Associates, Inc., 2019.
- 492 [28] C. Liu, L. Zhu, and M. Belkin. On the linearity of large non-linear models: when and why the
493 tangent kernel is constant. In H. Larochelle, M. Ranzato, R. Hadsell, M. Balcan, and H. Lin,
494 editors, *Advances in Neural Information Processing Systems*, volume 33, pages 15954–15964.
495 Curran Associates, Inc., 2020.
- 496 [29] P. M. Long. Properties of the after kernel. *CoRR*, abs/2105.10585, 2021.
- 497 [30] A. Madry, A. Makelov, L. Schmidt, D. Tsipras, and A. Vladu. Towards Deep Learning Models
498 Resistant to Adversarial Attacks. In *International Conference on Learning Representations*,
499 2018.
- 500 [31] P. Nakkiran. Adversarial robustness may be at odds with simplicity. *CoRR*, abs/1901.00532,
501 2019. URL <http://arxiv.org/abs/1901.00532>.
- 502 [32] T. Nguyen, R. Novak, L. Xiao, and J. Lee. Dataset distillation with infinitely wide convolutional
503 networks. In A. Beygelzimer, Y. Dauphin, P. Liang, and J. W. Vaughan, editors, *Advances in*
504 *Neural Information Processing Systems*, 2021.
- 505 [33] R. Novak, L. Xiao, J. Hron, J. Lee, A. A. Alemi, J. Sohl-Dickstein, and S. S. Schoenholz.
506 Neural tangents: Fast and easy infinite neural networks in python. In *8th International Con-*
507 *ference on Learning Representations, ICLR 2020, Addis Ababa, Ethiopia, April 26-30, 2020*.
508 OpenReview.net, 2020.
- 509 [34] G. Ortiz-Jiménez, S. Moosavi-Dezfooli, and P. Frossard. What can linearized neural networks
510 actually say about generalization? *CoRR*, abs/2106.06770, 2021.
- 511 [35] N. Papernot, P. D. McDaniel, and I. J. Goodfellow. Transferability in machine learning: from
512 phenomena to black-box attacks using adversarial samples. *CoRR*, abs/1605.07277, 2016.
- 513 [36] N. Papernot, P. D. McDaniel, I. J. Goodfellow, S. Jha, Z. B. Celik, and A. Swami. Practical
514 black-box attacks against machine learning. In R. Karri, O. Sinanoglu, A. Sadeghi, and X. Yi,
515 editors, *Proceedings of the 2017 ACM on Asia Conference on Computer and Communications*
516 *Security, AsiaCCS 2017, Abu Dhabi, United Arab Emirates, April 2-6, 2017*, pages 506–519.
517 ACM, 2017.
- 518 [37] N. Rahaman, A. Baratin, D. Arpit, F. Draxler, M. Lin, F. A. Hamprecht, Y. Bengio, and A. C.
519 Courville. On the spectral bias of neural networks. In K. Chaudhuri and R. Salakhutdinov,
520 editors, *Proceedings of the 36th International Conference on Machine Learning, ICML 2019,*
521 *9-15 June 2019, Long Beach, California, USA*, volume 97 of *Proceedings of Machine Learning*
522 *Research*, pages 5301–5310. PMLR, 2019.
- 523 [38] V. Shankar, A. Fang, W. Guo, S. Fridovich-Keil, J. Ragan-Kelley, L. Schmidt, and B. Recht.
524 Neural kernels without tangents. In H. D. III and A. Singh, editors, *Proceedings of the*
525 *37th International Conference on Machine Learning*, volume 119 of *Proceedings of Machine*
526 *Learning Research*, pages 8614–8623. PMLR, 13–18 Jul 2020.
- 527 [39] C. Simon-Gabriel, Y. Ollivier, L. Bottou, B. Schölkopf, and D. Lopez-Paz. First-order adversarial
528 vulnerability of neural networks and input dimension. In K. Chaudhuri and R. Salakhutdinov,
529 editors, *Proceedings of the 36th International Conference on Machine Learning, ICML 2019,*
530 *9-15 June 2019, Long Beach, California, USA*, volume 97 of *Proceedings of Machine Learning*
531 *Research*, pages 5809–5817. PMLR, 2019.

- 532 [40] J. M. Springer, M. Mitchell, and G. T. Kenyon. A little robustness goes a long way: Leveraging
533 robust features for targeted transfer attacks. In A. Beygelzimer, Y. Dauphin, P. Liang, and J. W.
534 Vaughan, editors, *Advances in Neural Information Processing Systems*, 2021.
- 535 [41] C. Szegedy, W. Zaremba, I. Sutskever, J. Bruna, D. Erhan, I. J. Goodfellow, and R. Fergus.
536 Intriguing properties of neural networks. In Y. Bengio and Y. LeCun, editors, *2nd International
537 Conference on Learning Representations, ICLR 2014, Banff, AB, Canada, April 14-16, 2014,
538 Conference Track Proceedings*, 2014.
- 539 [42] M. Tancik, P. P. Srinivasan, B. Mildenhall, S. Fridovich-Keil, N. Raghavan, U. Singhal, R. Ra-
540 mamoorathi, J. T. Barron, and R. Ng. Fourier features let networks learn high frequency functions
541 in low dimensional domains. In H. Larochelle, M. Ranzato, R. Hadsell, M. Balcan, and H. Lin,
542 editors, *Advances in Neural Information Processing Systems 33: Annual Conference on Neural
543 Information Processing Systems 2020, NeurIPS 2020, December 6-12, 2020, virtual*, 2020.
- 544 [43] D. Tsipras, S. Santurkar, L. Engstrom, A. Turner, and A. Madry. Robustness may be at odds
545 with accuracy. In *7th International Conference on Learning Representations, ICLR 2019, New
546 Orleans, LA, USA, May 6-9, 2019*, 2019.
- 547 [44] C.-H. Yuan and S.-H. Wu. Neural tangent generalization attacks. In M. Meila and T. Zhang,
548 editors, *Proceedings of the 38th International Conference on Machine Learning*, volume 139 of
549 *Proceedings of Machine Learning Research*, pages 12230–12240. PMLR, 18–24 Jul 2021.
- 550 [45] H. Zhang, Y. Yu, J. Jiao, E. P. Xing, L. E. Ghaoui, and M. I. Jordan. Theoretically principled
551 trade-off between robustness and accuracy. In K. Chaudhuri and R. Salakhutdinov, editors,
552 *Proceedings of the 36th International Conference on Machine Learning, ICML 2019, 9-15 June
553 2019, Long Beach, California, USA*, volume 97 of *Proceedings of Machine Learning Research*,
554 pages 7472–7482. PMLR, 2019.

555 Checklist

556 The checklist follows the references. Please read the checklist guidelines carefully for information on
557 how to answer these questions. For each question, change the default **[TODO]** to **[Yes]**, **[No]**, or
558 **[N/A]**. You are strongly encouraged to include a **justification to your answer**, either by referencing
559 the appropriate section of your paper or providing a brief inline description. For example:

- 560 • Did you include the license to the code and datasets? **[Yes]** See Section 4 and Appendix.
- 561 • Did you include the license to the code and datasets? **[No]** The code and the data are
562 proprietary.
- 563 • Did you include the license to the code and datasets? **[N/A]**

564 Please do not modify the questions and only use the provided macros for your answers. Note that the
565 Checklist section does not count towards the page limit. In your paper, please delete this instructions
566 block and only keep the Checklist section heading above along with the questions/answers below.

- 567 1. For all authors...
 - 568 (a) Do the main claims made in the abstract and introduction accurately reflect the paper’s
569 contributions and scope? **[Yes]**
 - 570 (b) Did you describe the limitations of your work? **[Yes]**
 - 571 (c) Did you discuss any potential negative societal impacts of your work? **[Yes]** Our work
572 sheds light properties of adversarial examples to make machine learning models more
573 reliable in the long run.
 - 574 (d) Have you read the ethics review guidelines and ensured that your paper conforms to
575 them? **[Yes]**
- 576 2. If you are including theoretical results...
 - 577 (a) Did you state the full set of assumptions of all theoretical results? **[Yes]**
 - 578 (b) Did you include complete proofs of all theoretical results? **[Yes]**

- 579 3. If you ran experiments...
- 580 (a) Did you include the code, data, and instructions needed to reproduce the main experi-
581 mental results (either in the supplemental material or as a URL)? [Yes]
- 582 (b) Did you specify all the training details (e.g., data splits, hyperparameters, how they
583 were chosen)? [Yes]
- 584 (c) Did you report error bars (e.g., with respect to the random seed after running experi-
585 ments multiple times)? [Yes]
- 586 (d) Did you include the total amount of compute and the type of resources used (e.g., type
587 of GPUs, internal cluster, or cloud provider)? [Yes]
- 588 4. If you are using existing assets (e.g., code, data, models) or curating/releasing new assets...
- 589 (a) If your work uses existing assets, did you cite the creators? [Yes]
- 590 (b) Did you mention the license of the assets? [Yes]
- 591 (c) Did you include any new assets either in the supplemental material or as a URL? [Yes]
- 592 (d) Did you discuss whether and how consent was obtained from people whose data you're
593 using/curating? [N/A]
- 594 (e) Did you discuss whether the data you are using/curating contains personally identifiable
595 information or offensive content? [N/A]
- 596 5. If you used crowdsourcing or conducted research with human subjects...
- 597 (a) Did you include the full text of instructions given to participants and screenshots, if
598 applicable? [N/A]
- 599 (b) Did you describe any potential participant risks, with links to Institutional Review
600 Board (IRB) approvals, if applicable? [N/A]
- 601 (c) Did you include the estimated hourly wage paid to participants and the total amount
602 spent on participant compensation? [N/A]